

Supporting Information

Effect of phenyl group on non-linear optical (NLO) and aggregation induced emission (AIE) studies of ferrocene conjugated linear D- π -A/ D- π -A- π -A chromophores

Thamodharan Viswanathan^a, Ezhumalai David^a, Selvam Prabu^a, Kamini Mishra^a, Muthuramalingam Prakash^c, Swaminathan Shanmugan^c, Nallasamy Palanisami^{ab*}

- a. Department of Chemistry, School of Advanced Sciences, Vellore Institute of Technology, Vellore - 632014, Tamil Nadu, India.
- b. Centre for Functional Materials, Vellore Institute of Technology, Vellore - 632014, Tamil Nadu, India.
- c. Department of Chemistry, SRM Institute of Science and Technology, Kattankulathur - 603203, Tamil Nadu, India.

* Corresponding Author: Email: palanisami.n@gmail.com; palanisami.n@vit.ac.in; Tel: +91 9842639776.

Experimental

Materials and Procedures

The chromophores **1-4** were synthesized using the Knoevenagel condensation reaction. All the chemicals and solvents were purchased from Aldrich Chemicals and TCI chemicals. Chemicals were used without further purification and the solvents were distilled prior to use. Ferrocene phenyl^[1] and biphenyl aldehydes^[2] were prepared by previous reports.

General Physical Measurements

The NMR spectra were recorded on a BRUKER (400 MHz) spectrometer. Chemical shifts were reported in δ (ppm), and ESI-mass spectra were recorded under LC/MS, 6230B Time of Flight (TOF), Agilent technologies. Micro-elemental analyses were determined by PERKIN-ELMER CHN-2400. UV-Visible spectra were recorded using Agilent 8453 UV-Visible diode array spectrophotometer using the chloroform solvent. All Steady-state photoluminescence (PL) measurements were performed using Edinburg FLS 980, spectrometer. PL decay dynamics of chromophores **1-4**, AIE-active state emissions were measured using a picosecond xenon Arc lamp of 450 W power. PL decay measurements for lifetimes were carried out on a TCSPC setup from Edinburgh Instruments using 371 nm Picosecond Pulsed Diode Laser (UK, EPL-375) and analysis was done with F980 software. Electrochemical measurements were performed on a CH-Instruments model CHI620E, using an oxygen-free one-compartment cell using a glassy carbon electrode as the working electrode, a saturated Ag/AgCl as the reference electrode and a platinum wire as an auxiliary electrode. CHCl_3 was used as a solvent and $[\text{N}(\text{C}_4\text{H}_9\text{-n})_4] \text{ClO}_4$ used as a supporting electrolyte containing ca. 10^{-3} M analyte (0.1 M $[\text{N}(\text{C}_4\text{H}_9\text{-n})_4] \text{ClO}_4$). All $E_{1/2}$ values were calculated from $(E_{\text{pa}} + E_{\text{pc}})/2$ (p_a – anodic potential and p_c – cathodic potential) at a scan rate of 0.05 mV s^{-1} .

Crystal structure determination

The crystal structure of chromophores **2** and **4** was obtained by the slow evaporation method in ethyl acetate/hexane (1:3) mixture, and both are crystallized in reddish yellow-colored crystals. The crystal was stored in paraffin oil and mounted in a MiTe-Genloop, and measured at 296 K. The crystal measurement was made on a Bruker Kappa Apex II coupled with a CCD area detector with graphite-monochromated with $M_o K_\alpha$ radiation (0.71073 \AA). The crystal, with an approximate size of $0.350 \times 0.350 \times 0.300 \text{ mm}$, was mounted on a glass loop. It was solved by direct methods and expanded using Fourier techniques. All calculations were

performed using the crystallographic software package X shell. The Apex2 package was used for cell refinements and data reductions.^[3] The structures were solved by direct methods using the SHELXS 97^[4] program with the Olex2 graphical user interface.^[5] Structural refinements were carried out using SHELXL-2014.^[6] The positions of all the atoms were obtained by direct method and the crystallographic details are summarized in Table S1.

Determination of Molar Absorption Coefficient

The molar extinction coefficients (ϵ) were determined according to the Beer-Lambert Law equation,

$$A = \epsilon l c \dots\dots\dots(1)$$

Where A is the absorbance, c is the concentration and l is the cuvette path length.

Diffuse Reflectance Spectroscopic (DRS) method

The diffuse reflectance spectroscopic (DRS) methods were used in the wavelength range of 200–1500 nm. The solid-state absorption cut-off wavelength of chromophores exhibits at 549 (1), 527 (2), 571 (3) and 647 nm (4) were shown in Fig.S17-S18. The band gap values of the chromophores 1 -4 were determined using Eqn (2),

$$h\nu = (h\nu - E_g)^{1/2} \dots\dots\dots (2)$$

Where A is a constant, h stands for Planck's constant and ν is the frequency of the incident photons. The energy band gap value was obtained from a Tauc plot $[(\alpha h\nu)^2 \text{ vs. } h\nu]$. The intersection of the line on the photon energy axis drawn from the maximum absorption endpoint of the curve was considered as the energy band gap. The corresponding band gap value of chromophores 3.98, 3.67, 3.71 and 3.57 eV for 1-4 respectively (Fig. S16).

Electrochemical Parameters

The cyclic voltammetric data such as anodic peak potential (E_a), anode current (i_a), cathodic peak potential (E_c), and cathode current (i_c) were observed and also the half-wave potential ($E_{1/2}$), peak separation (ΔE) and current ratio (i_c/i_a) were calculated using the appropriate equations as follows and the parameter was shown in Table S4.

$$E_{1/2} = (E_{pa} + E_{pc})/2 \dots\dots\dots (3)$$

$$\Delta E = E_{pa} - E_{pc} \dots\dots\dots (4)$$

Computational calculation details

The density functional theory (DFT) based calculations were performed for understanding the structural and functional features. Further, DFT functional and combination of the basis set support to definition of bonding patterns, electronic charge, and molecular orbital energy distribution. The dipole moment of the NLO chromophores at excited states were calculated using the single-excitation configuration interaction method with the time-dependent - DFT (TD-DFT) method, which uses to investigate the origin of electronic absorption spectra and nonlinear optical properties. The geometries of chromophores **1 - 4** in gas and the solution phase were optimized using Becke's three-parameter and Lee–Yang–Parr functional (B3LYP). The B3LYP functional is combined with the 6-31+G** basis set for all the calculations. On the optimized geometries, TD-DFT single-point calculations have been carried out using the B3LYP/6-31+G** level of theory. All the computations were performed using the G16 package. The electronic geometries and frontier molecular orbital structures were taken using the Gauss View 6.1.1 molecular visualization program.^[7-9]

Polarizability and Hyperpolarizability

The molecular polarizability of the chromophores depends on the efficiency of electronic communication between donor and acceptor groups, playing a key role in determining the intra-molecular charge transfer. The results of polarizability and first hyperpolarizabilities were calculated with the DFT/B3LYP/6-31+G** level of theory. The values of the first hyperpolarizability (β), dipole moment (μ), and polarizability (α) of chromophores **1-4** are reported in the atomic mass units (a.u) and electrostatic unit (esu). The first hyperpolarizability is a third rank tensor that can be described by $3 \times 3 \times 3$ matrix. The components of β are defined as the coefficients in the Taylor series expansion of the energy in the external electric field. When the external electric field is weak and homogeneous, this expansion becomes

$$E = E^0 - \mu_a F_a - 1/2 \alpha_{\alpha\beta} F_\alpha F_\beta - 1/6 \beta_{\alpha\beta\gamma} F_\alpha F_\beta F_\gamma + \dots \quad (5)$$

where E^0 is the energy of the unperturbed molecules, F_a is the field at the rigid, μ_a , $\alpha_{\alpha\beta}$ and $\beta_{\alpha\beta\gamma}$ are the components of dipole moment, polarizability and the first order hyperpolarizabilities respectively. For calculating the magnitude of total static dipole moment (μ_{tot}), the mean polarizability (α_0) and the mean first hyperpolarizability (β_0) are followed as given in the literature.^[9-11] The mean polarizability is defined as the following equation

$$\alpha_0 = (\alpha_{xx} + \alpha_{yy} + \alpha_{zz})/3 \dots \quad (6)$$

The components of the first hyperpolarizability can be calculated using the following equation.

$$\beta_0 = (\beta_x^2 + \beta_y^2 + \beta_z^2)^{1/2} \dots\dots\dots (7)$$

where, $\beta_x = \beta_{xxx} + \beta_{yyy} + \beta_{zzz}$; $\beta_y = \beta_{yyy} + \beta_{yzz} + \beta_{yxx}$; $\beta_z = \beta_{zzz} + \beta_{zxx} + \beta_{zyy}$ complete equation for calculating the magnitude of β_0 . The total dipole moment can be calculated using the following equation.

$$\mu_t = (\mu_x^2 + \mu_y^2 + \mu_z^2)^{1/2} \dots\dots\dots (8)$$

General procedure for the synthesis of chromophores 1-4

An equimolar ratio of mono or biphenyl ferrocene substituted aldehydes (1 mmol), cyanovinylenes [(1 mmol) Malanonitrile, 4-nitrophenylacetonitrile] were dissolved in toluene (10 ml) and a few drops of piperidine were added and refluxed for 3h. Then, the solvent was removed using a rotary evaporator and the residue was poured into water and separated using DCM (15 ml \times 2). The crude product was purified by column chromatography (hexane/ethyl acetate, 30%) to yield chromophores 1-4.

Chromophore-1, Yield (65.3%), MP = 163-165 °C, Anal.Calc. for: C₂₀H₁₄FeN₂ (M. wt = 338.19), Cal; C, 71.03; H, 4.17; N, 8.28: Found; C, 69.85; H, 4.05; N, 8.17. ¹H NMR (400 MHz, CDCl₃, ppm, TMS): δ = 7.72 (s, 1H, -CH=), 7.57 (q, 4H, J =8.4 Hz, C₆H₄), 4.69 (s, 2H, H _{α} C₅H₄), 4.42 (s, 2H, H _{β} C₅H₄), 4.05 (s, 5H, C₅H₅). ¹³C NMR (100 MHz, CDCl₃, ppm, TMS): δ = 159.2 (1C, -CH=), 145.6 (1C, p -C₆H₄), 132.2 (2C, o -C₆H₄), 126.2 (3C, p,m -C₆H₄), 119.4 (2C, CN), 108.8 (1C, C-CN₂), 82.4 (1C, C _{$ipso$}), 70.2 (2C, C _{β} C₅H₄), 69.9 (5C, C₅H₅), 66.9 (2C, C _{α} C₅H₄). LC-mass (m/z) exact mass: 338.0506, observed mass: 338.0500. UV-vis (CHCl₃, nm, ϵ , cm⁻¹M⁻¹): 298, 365, 459. Fluorescence (CHCl₃); λ_{ex} (255) = 326 nm.

Chromophore-2, Yield (68.5%), MP = 205-207 °C, Anal.Calc. for: C₂₅H₁₈FeN₂O₂ (M. wt = 434.27), Cal; C, 69.14; H, 4.18; N, 6.45: Found; C, 68.85; H, 4.16; N, 6.19. ¹H NMR (400 MHz, CDCl₃, ppm, TMS): δ = 8.32 (d, 2H, J =8.8 Hz, m -C₆H₄), 7.91 (d, 2H, J =8.0 Hz, o -C₆H₄), 7.87 (d, 2H, J = 8.8 Hz, m -C₆H₄), 7.63 (s, 1H, -CH=), 7.59 (d, 2H, J = 8.4 Hz, o -C₆H₄), 4.75 (s, 2H, H _{α} C₅H₄), 4.45 (s, 2H, H _{β} C₅H₄), 4.07 (s, 5H, C₅H₄). ¹³C NMR (100 MHz, CDCl₃, ppm, TMS): δ = 147.6 (1C, -CH=), 145.3 (2C, p -C₆H₄), 144.7 (1C, p -C₆H₄) 141.1 (1C), 130.2-130.1 (2C, o -C₆H₄), 126.5 (2C, m -C₆H₄), 126.3 (2C, o -C₆H₄), 124.4 (2C, m -C₆H₄), 117.7 (1C, CN), 107.4 (1C, C-CN), 83.1 (1C, C _{$ipso$}), 70.1 (2C, C _{β} C₅H₄), 69.9 (5C, C₅H₅), 66.9 (2C, C _{α} C₅H₄). LC-mass (m/z) exact mass: 434.0718, observed mass: 434.0709. UV-vis (CHCl₃, nm, ϵ , cm⁻¹M⁻¹): 248, 366, 508. Fluorescence (CHCl₃); λ_{ex} (255) = 331 nm.

Chromophore-3, Yield (60.8%), MP = 185-187 °C, Anal.Calc. for: C₂₆H₁₈FeN₂ (M. wt = 414.28), Cal; C, 75.38; H, 4.38; N, 6.76: Found; C, 74.85; H, 4.26; N, 6.49. ¹H NMR (400 MHz, CDCl₃, ppm, TMS): δ = 7.64 (s, 1H, -CH=), 7.59 (d, 2H, *J* = 7.2 Hz, C₆H₄), 7.47 (d, 4H, *J* = 5.4 Hz, C₆H₄), 7.34 (d, 2H, *J* = 7.2 Hz, C₆H₄), 4.62 (s, 2H, H_α C₅H₄), 4.28 (s, 2H, H_β C₅H₄), 4.00 (s, 5H, C₅H₅). ¹³C NMR (100 MHz, CDCl₃, ppm, TMS): δ = 148.1 (1C, -CH=), 141.5 (1C, *p*-C₆H₄), 139.1 (1C, *p*-C₆H₄), 137.5 (1C, *p*-C₆H₄), 131.6 (1C, *p*-C₆H₄), 129.6 (2C, *m*-C₆H₄), 127.6 (2C, *m*-C₆H₄), 126.9 (2C, *m*-C₆H₄), 126.6 (2C, *o*-C₆H₄), 112.2 (2C, CN), 103.3 (1C, C-CN₂), 84.7 (1C, C_{ipso}), 69.7 (2C, C₅H₅), 69.2 (2C, C_β C₅H₄), 66.6 (5C, C_α C₅H₄). LC-mass (m/z) exact mass: 414.0819, observed mass: 414.0703. UV-vis (CHCl₃, nm, ε, cm⁻¹M⁻¹): 306, 356, 468. Fluorescence (CHCl₃); λ_{ex} (255) = 335 nm.

Chromophore-4, Yield (75.4%), MP = >300 °C decomposes, Anal.Calc. for: C₃₁H₂₂FeN₂O₂ (M. wt = 510.37), Cal; C, 72.95; H, 4.35; N, 5.49. Found, C, 72.45; H, 4.26; N, 5.17. ¹H NMR (400 MHz, CDCl₃, ppm, TMS): δ = 8.33 (d, 2H, *J* = 8.87 Hz, *m*-C₆H₄), 8.05 (d, 2H, *J* = 8.0 Hz, *o*-C₆H₄), 7.88 (d, 2H, *J* = 8.8 Hz, *m*-C₆H₄), 7.79 (d, 2H, *J* = 8.4 Hz, *o*-C₆H₄), 7.71 (s, 1H, -CH=), 7.59 (s, 4H, C₆H₄), 4.71 (s, 2H, H_α C₅H₄), 4.38 (s, 2H, H_β C₅H₄), 4.08 (s, 5H, C₅H₅). ¹³C NMR (100 MHz, CDCl₃, ppm, TMS): δ = 147.8 (1C, -CH=), 145.1 (1C, *p*-C₆H₄), 144.1 (1C, *p*-C₆H₄), 140.8 (1C, *p*-C₆H₄), 140.0 (1C, *p*-C₆H₄), 136.7 (1C, *p*-C₆H₄), 131.5 (1C, *p*-C₆H₄), 130.5 (2C, *m*-C₆H₄), 127.2-126.7 (6C, C₆H₄), 126.6 (2C, *o*-C₆H₄), 124.4 (2C, *m*-C₆H₄), 117.5 (1C, CN), 108.6 (1C, C-CN), 84.4 (1C, C_{ipso}), 69.8 (5C, C₅H₅), 69.4 (2C, C_α C₅H₄), 66.6 (2C, C_β C₅H₄). LC-mass (m/z) exact mass: 510.1031, observed mass: 510.1020. UV-vis (CHCl₃, nm, ε, cm⁻¹M⁻¹): 271, 371, 520. Fluorescence (CHCl₃); λ_{ex} (255) = 338 nm.

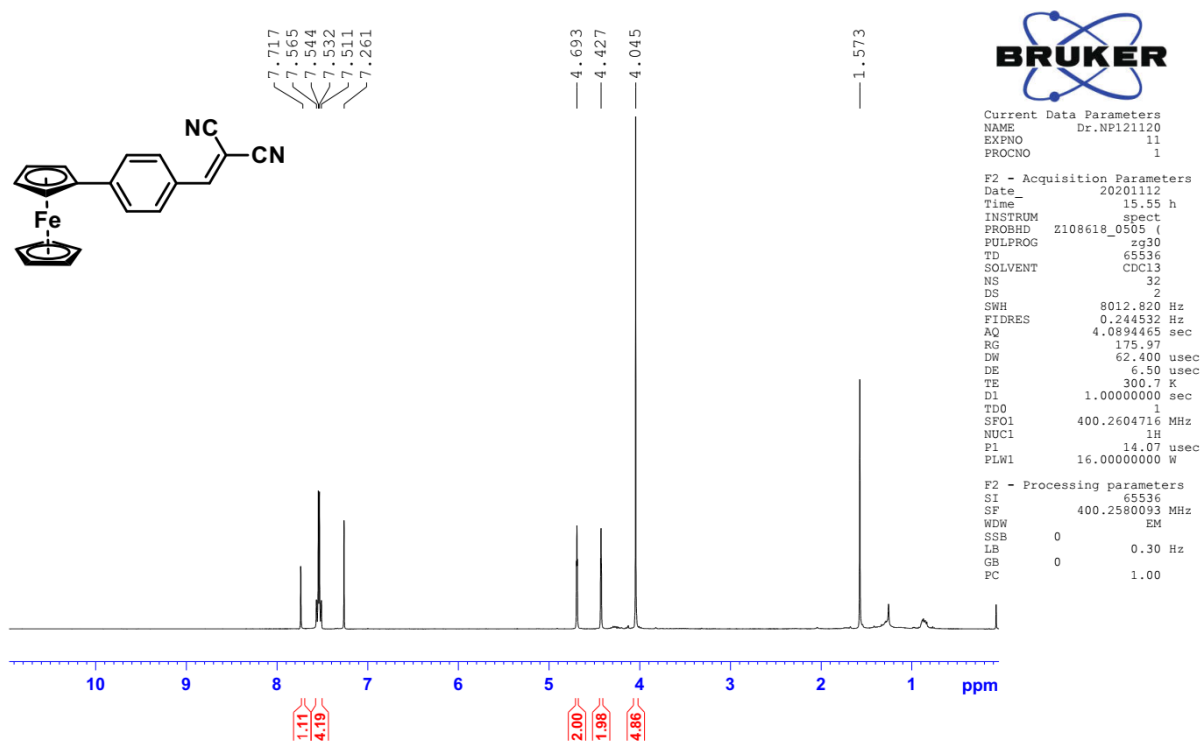


Fig. S1 ¹H NMR spectrum of chromophore 1 in CDCl₃.

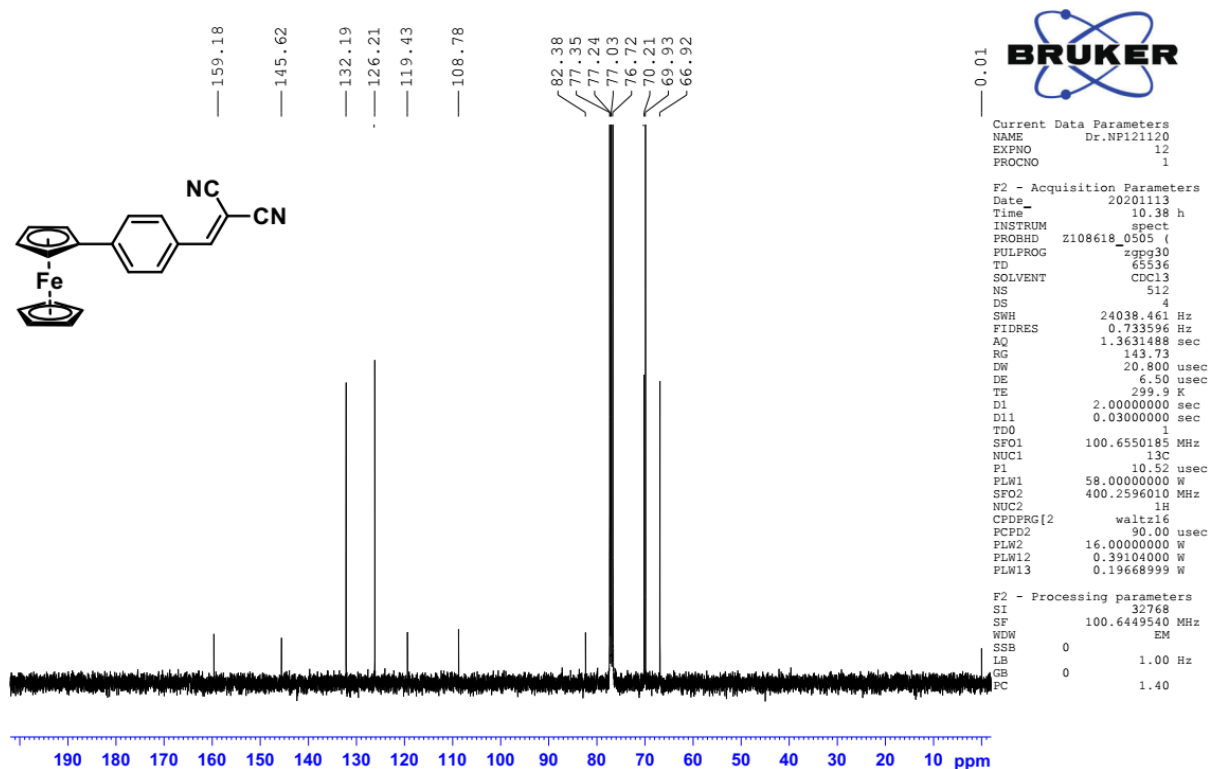


Fig. S2 ¹³C NMR spectrum of chromophore 1 in CDCl₃.

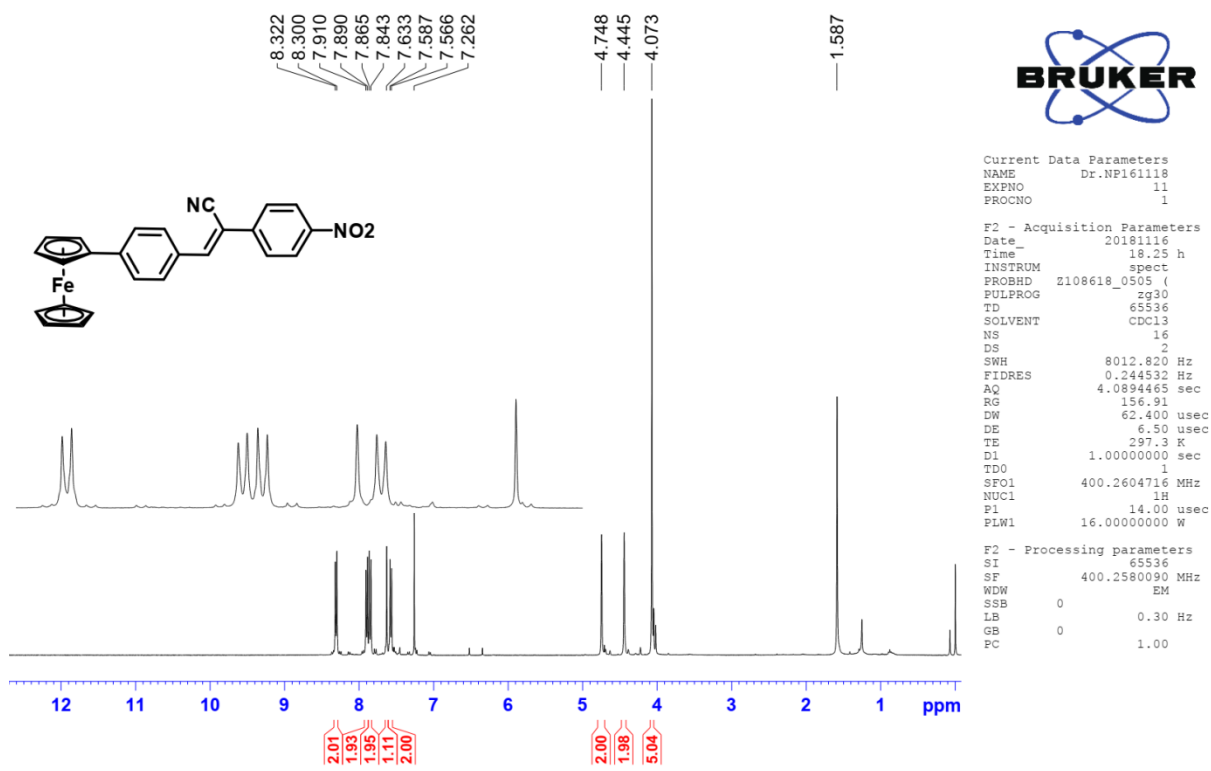


Fig. S3 ¹H NMR spectrum of chromophore 2 in CDCl₃.

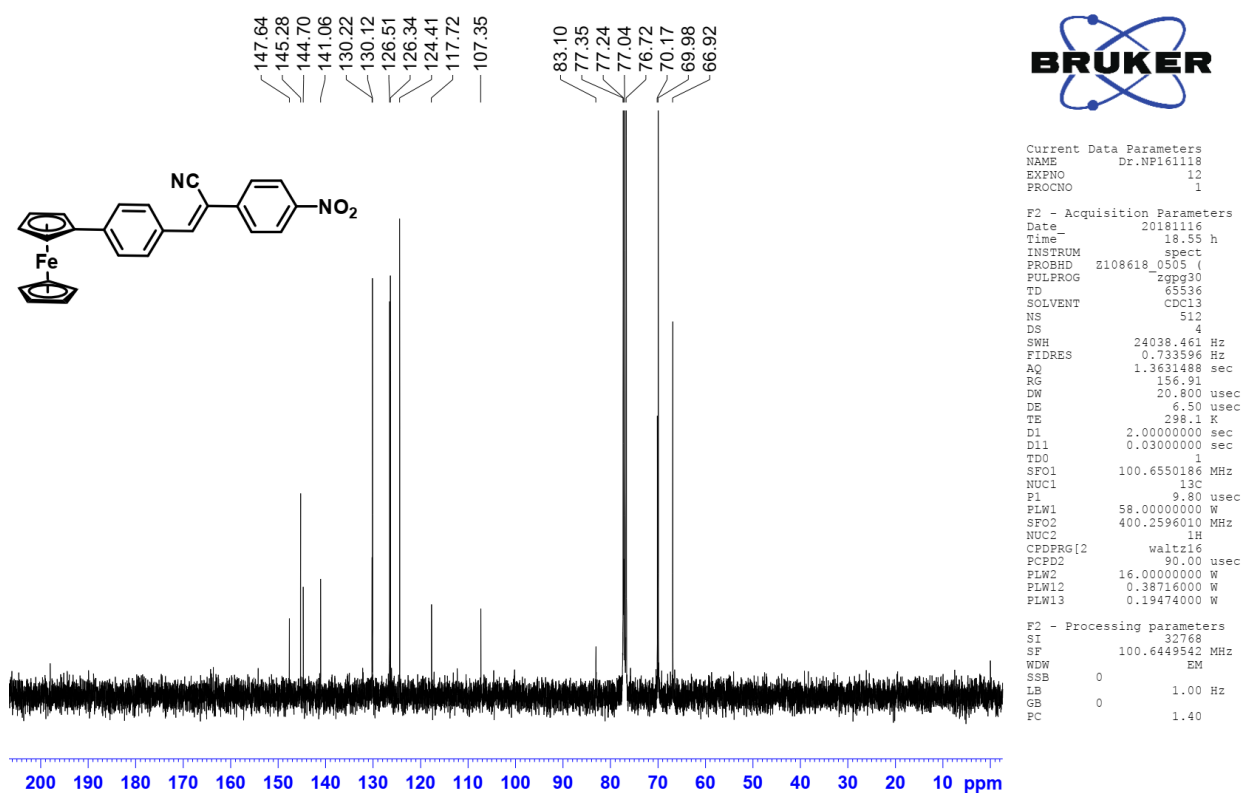
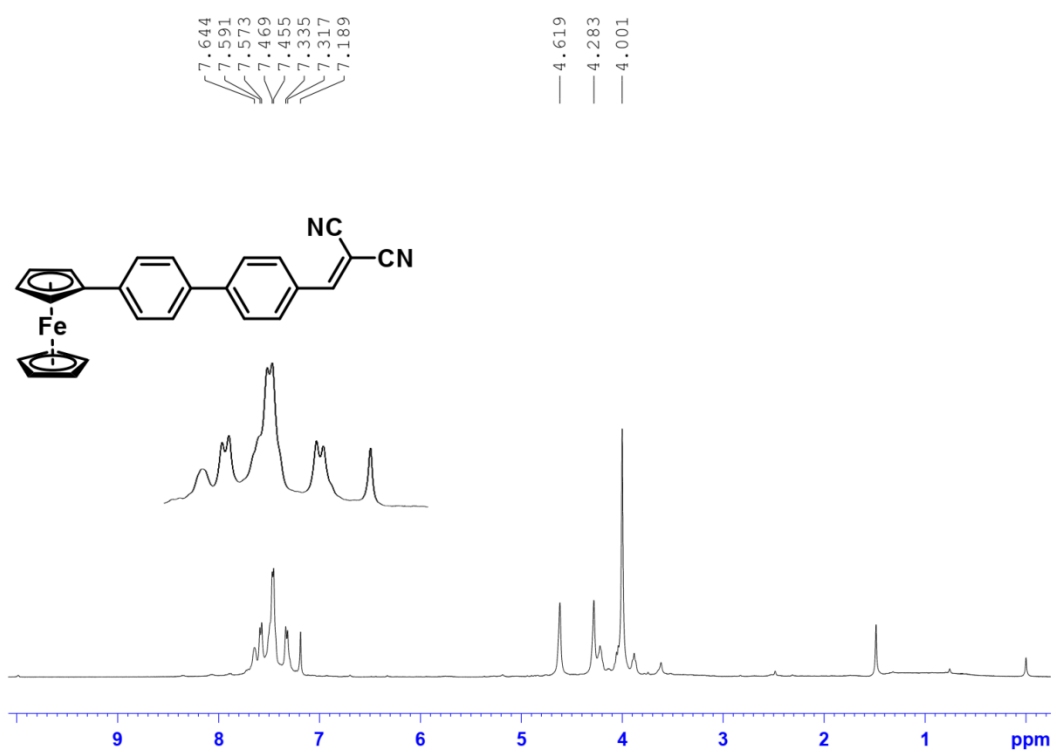


Fig. S4 ¹³C NMR spectrum of chromophore 2 in CDCl₃.

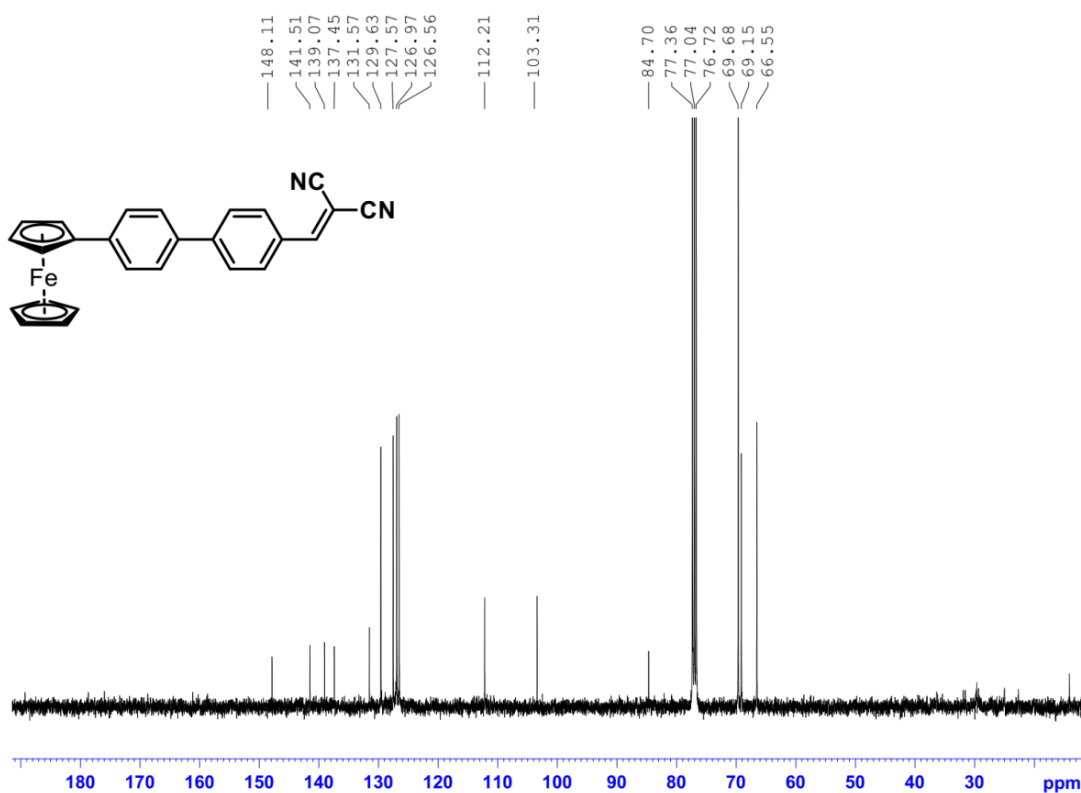


Current Data Parameters
NAME NMR PH2CN
EXPNO 2
PROCNO 1

F2 - Acquisition Parameters
Date_ 20201106
Time 16.40 h
INSTRUM spect
PROBHD z108618_0505 ()
PULPROG zg30
TD 65536
SOLVENT CDCl3
NS 32
DS 2
SWH 8012.820 Hz
FIDRES 0.244532 Hz
AQ 4.0894465 sec
RG 127.79
DW 62.400 usec
DE 6.50 usec
TE 299.9 K
D1 1.0000000 sec
TDO 1
SFO1 400.2604716 MHz
NUC1 1H
P1 14.07 usec
PLW1 16.0000000 W

F2 - Processing parameters
SI 65536
SF 400.2604716 MHz
WDW EM
SSB 0
LB 0.30 Hz
GB 0
PC 1.00

Fig. S5 ¹H NMR spectrum of chromophore-3 in CDCl₃.



Current Data Parameters
NAME Dr.NF121120
EXPNO 14
PROCNO 1

F2 - Acquisition Parameters
Date_ 20201113
Time 0.15 h
INSTRUM spect
PROBHD z108618_0505 ()
PULPROG zgpg30
TD 65536
SOLVENT CDCl3
NS 512
DS 4
SWH 24038.461 Hz
FIDRES 0.733596 Hz
AQ 1.3631488 sec
RG 175.97
DW 20.800 usec
DE 6.50 usec
TE 300.5 K
D1 2.0000000 sec
D11 0.0300000 sec
TDO 1
SFO1 100.6250185 MHz
NUC1 13C
P1 10.52 usec
PLW1 58.0000000 W
SFO2 400.2596010 MHz
NUC2 1H
CPDPRG2 waltz16
PCPD2 90.00 usec
PLW2 16.0000000 W
PLW12 0.39104000 W
PLW13 0.19668999 W

F2 - Processing parameters
SI 32768
SF 100.6250185 MHz
WDW EM
SSB 0
LB 1.00 Hz
GB 0
PC 1.40

Fig. S6 ¹³C NMR spectrum of chromophore-3 in CDCl₃.

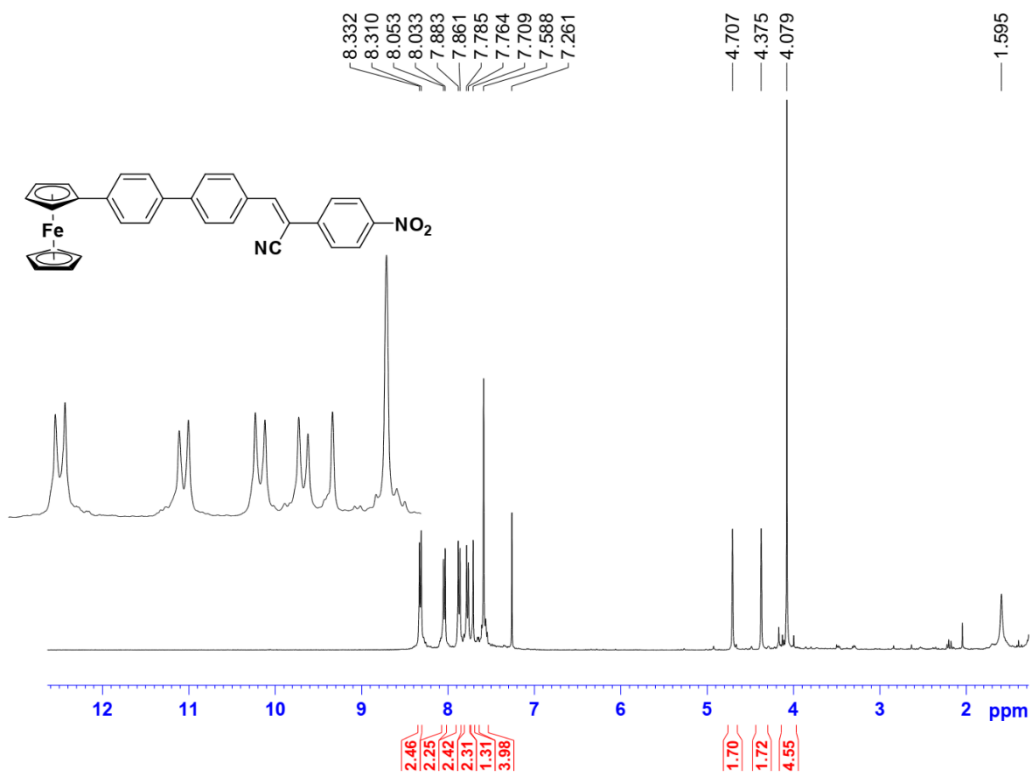


Fig. S7 ¹H NMR spectrum of chromophore-4 in CDCl₃.

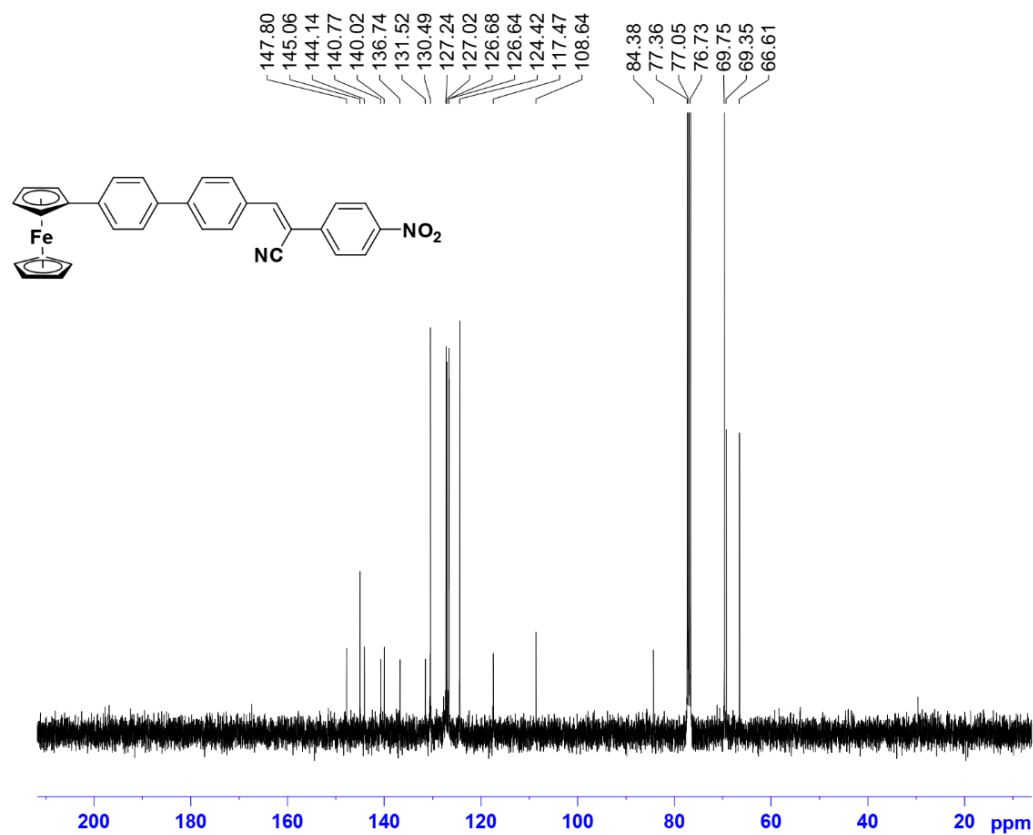


Fig. S8 ¹³C NMR spectrum of chromophore-4 in CDCl₃.

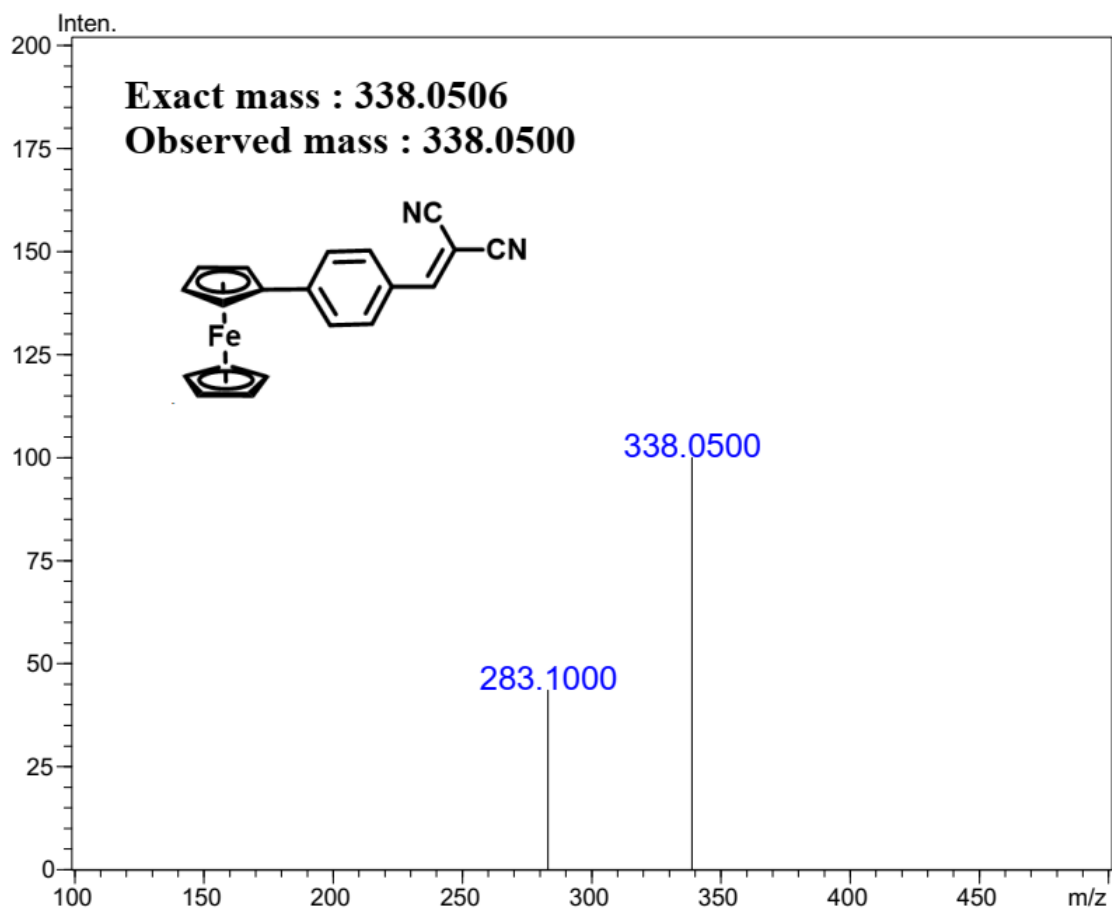


Fig. S9 LC-MS spectrum of chromophore-1.

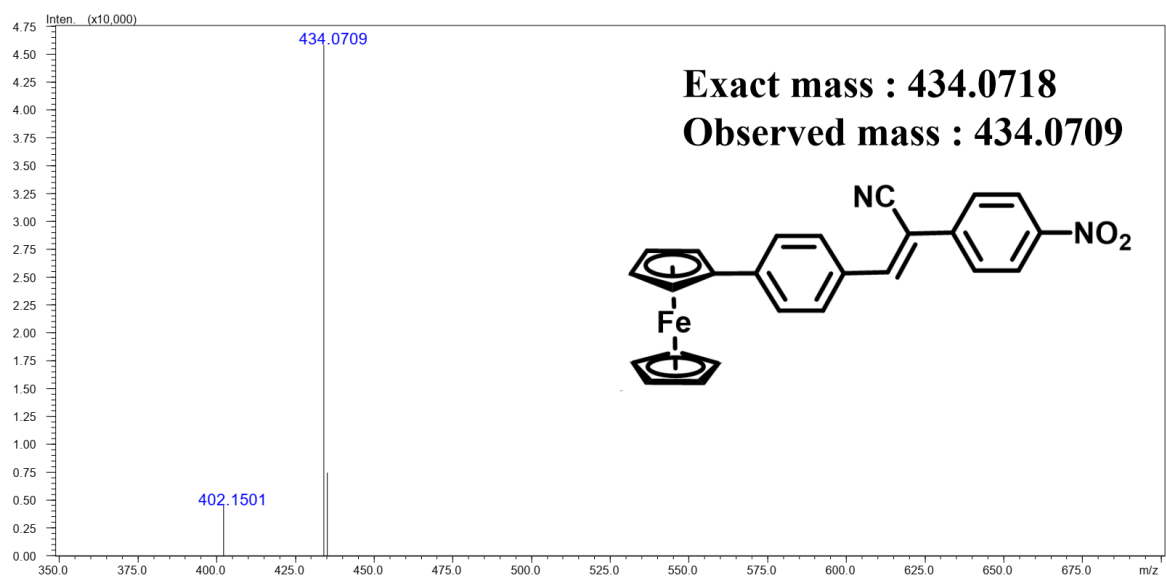


Fig. S10 LC-MS spectrum of chromophore-2.

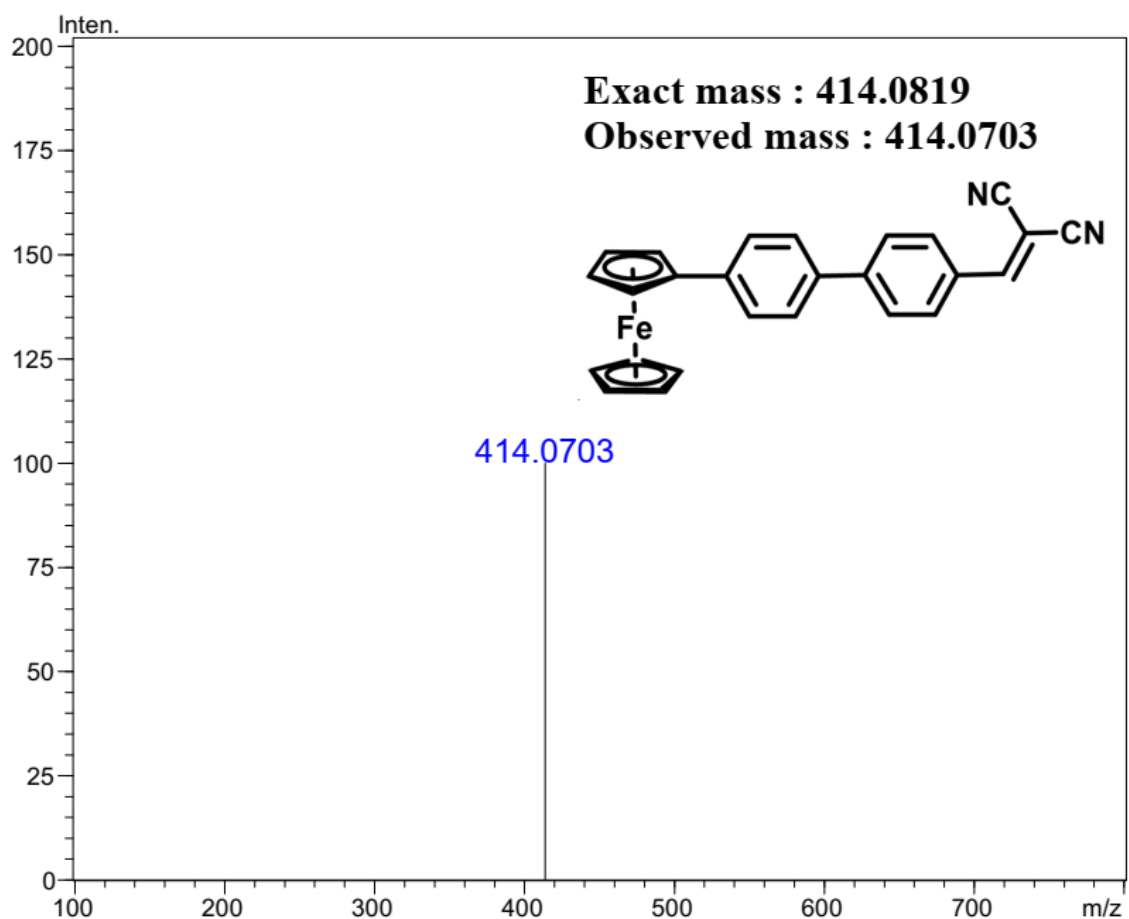


Fig. S11 LC-MS spectrum of chromophore-3.

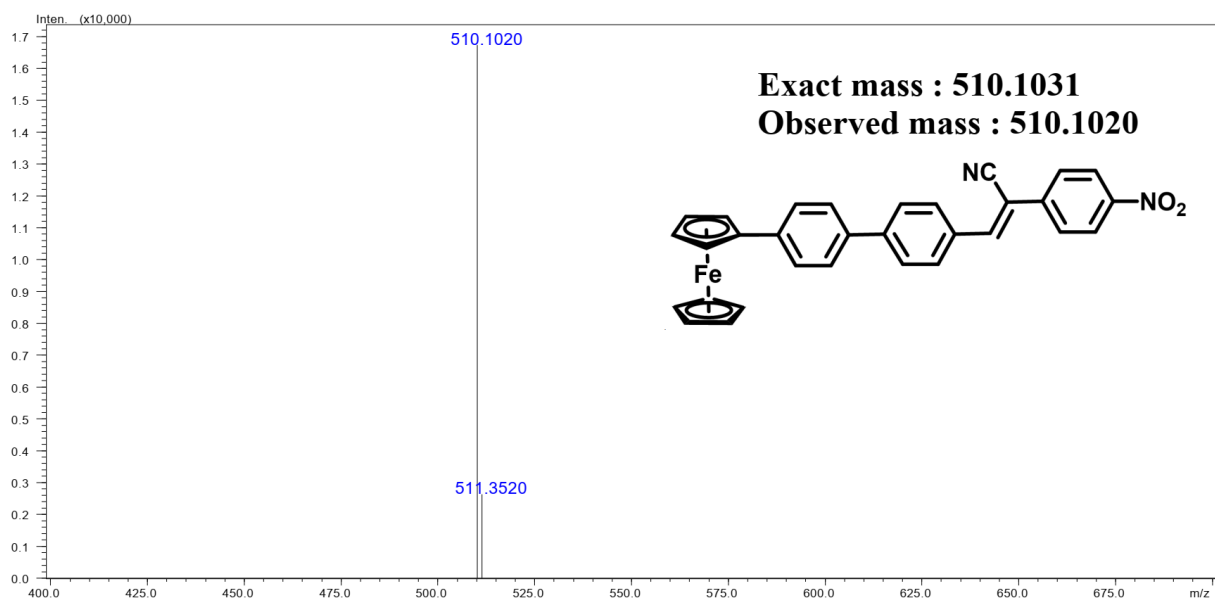


Fig. S12 LC-MS spectrum of chromophore-4.

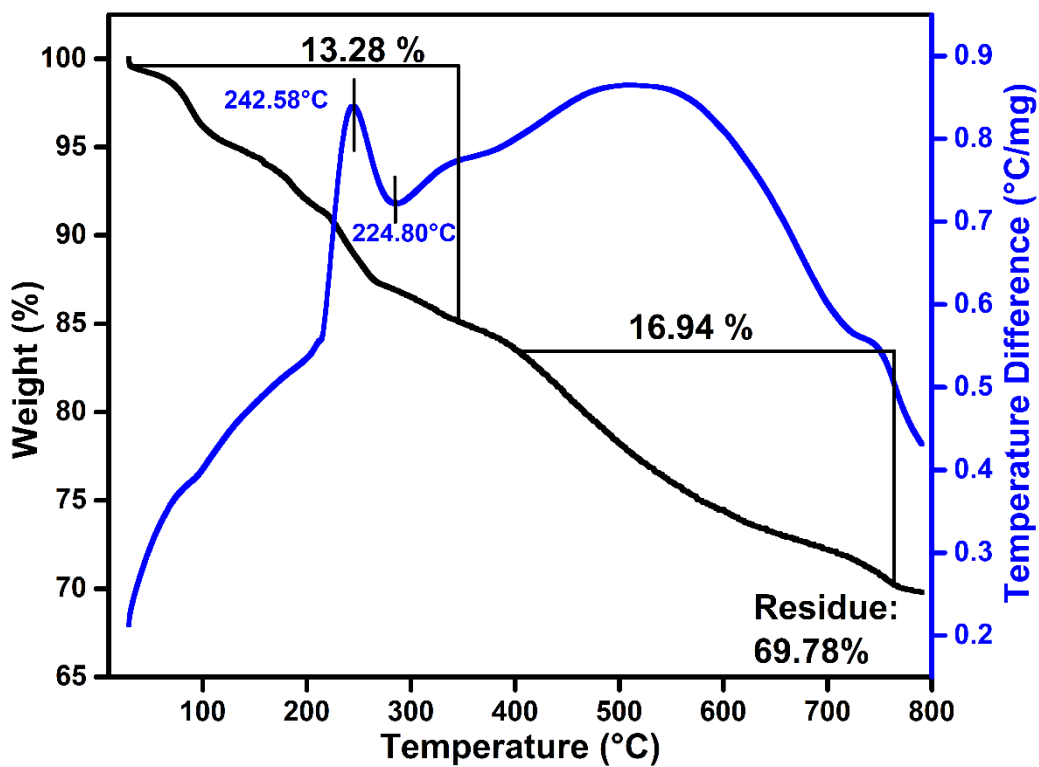


Fig. S13 TGA/DSC spectra of chromophore 2.

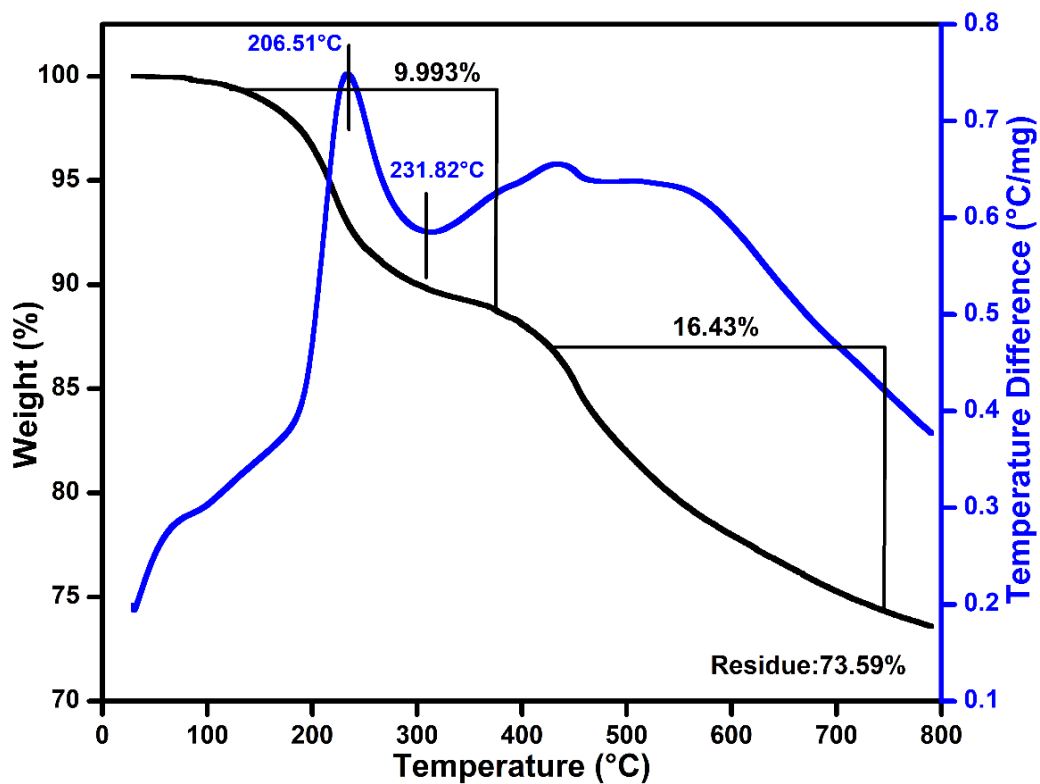


Fig. S14. TGA/DSC spectra of chromophore 4.

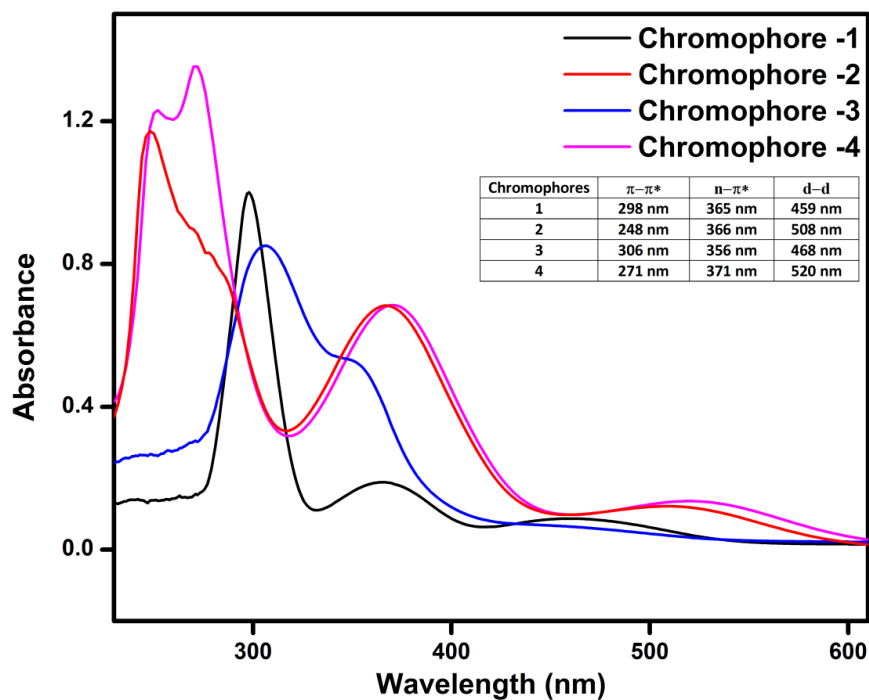


Fig. S15. UV-Vis absorption spectra of chromophores 1 - 4 in CHCl_3 (1×10^{-5} M).

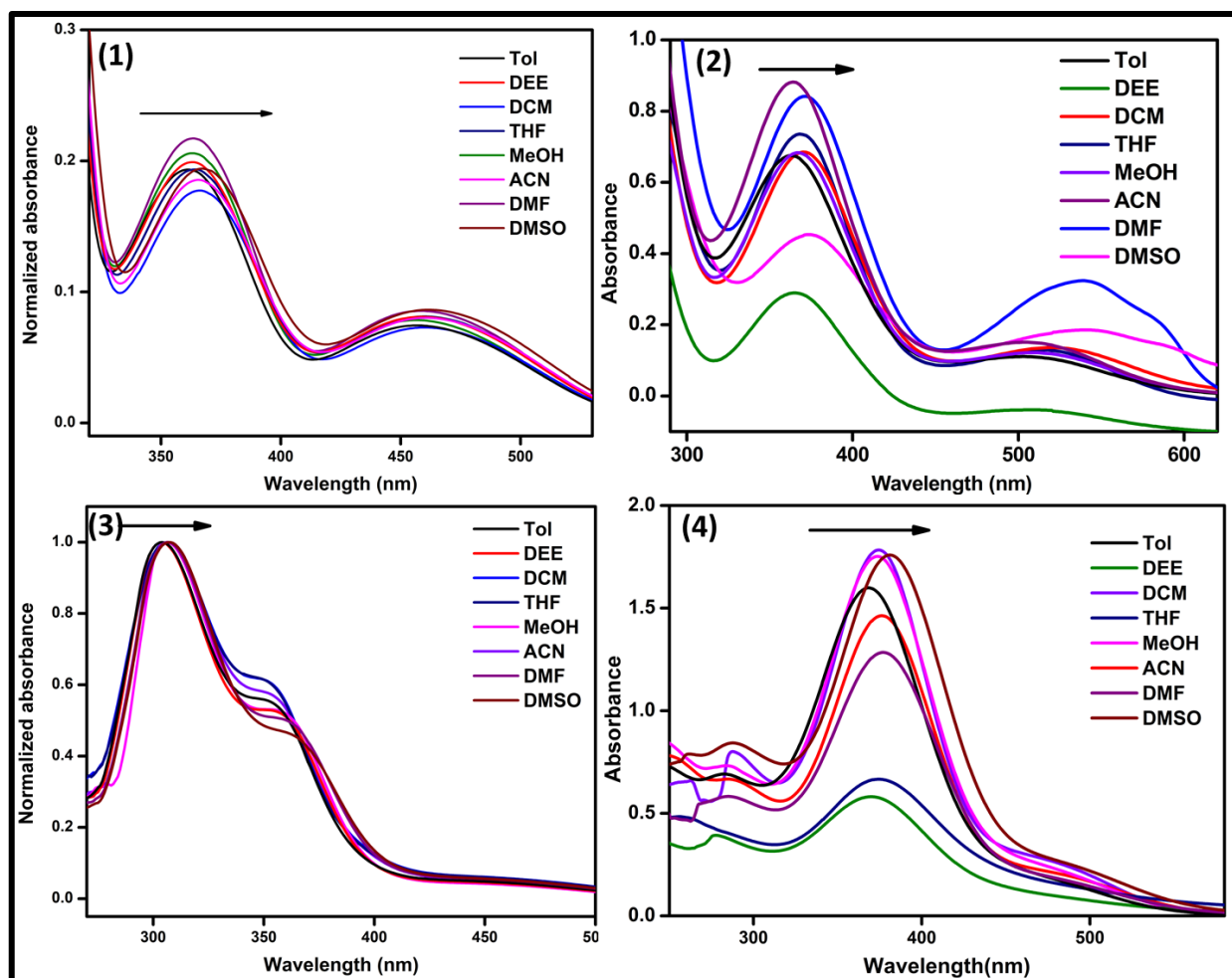


Fig. S16. Absorption properties of chromophores 1 - 4 in different polarity solvents (1×10^{-5} M).

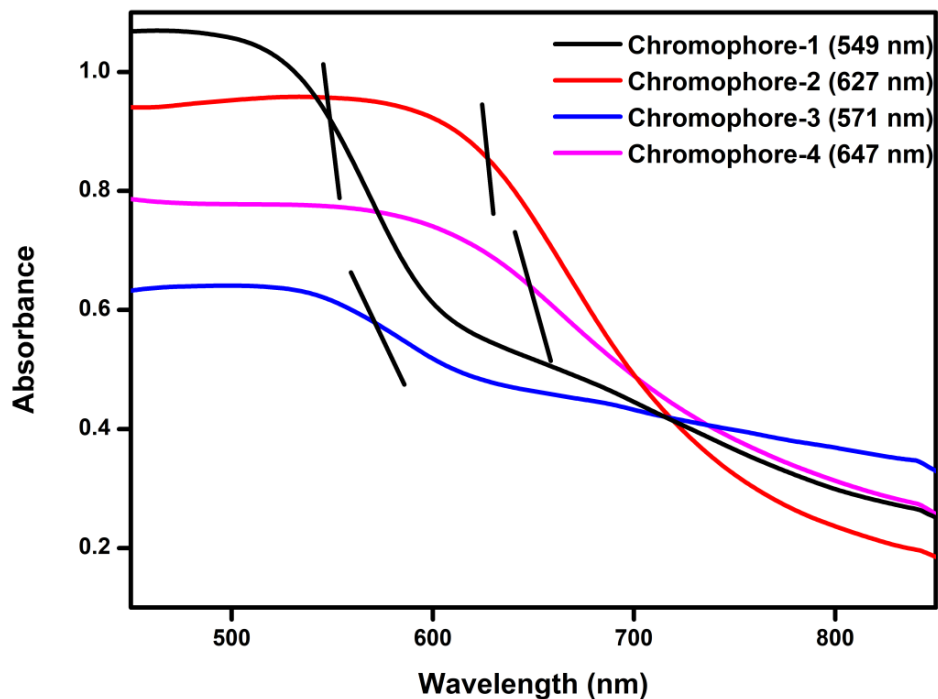


Fig. S17 Solid state UV-vis absorption spectra of chromophores 1 and 2.

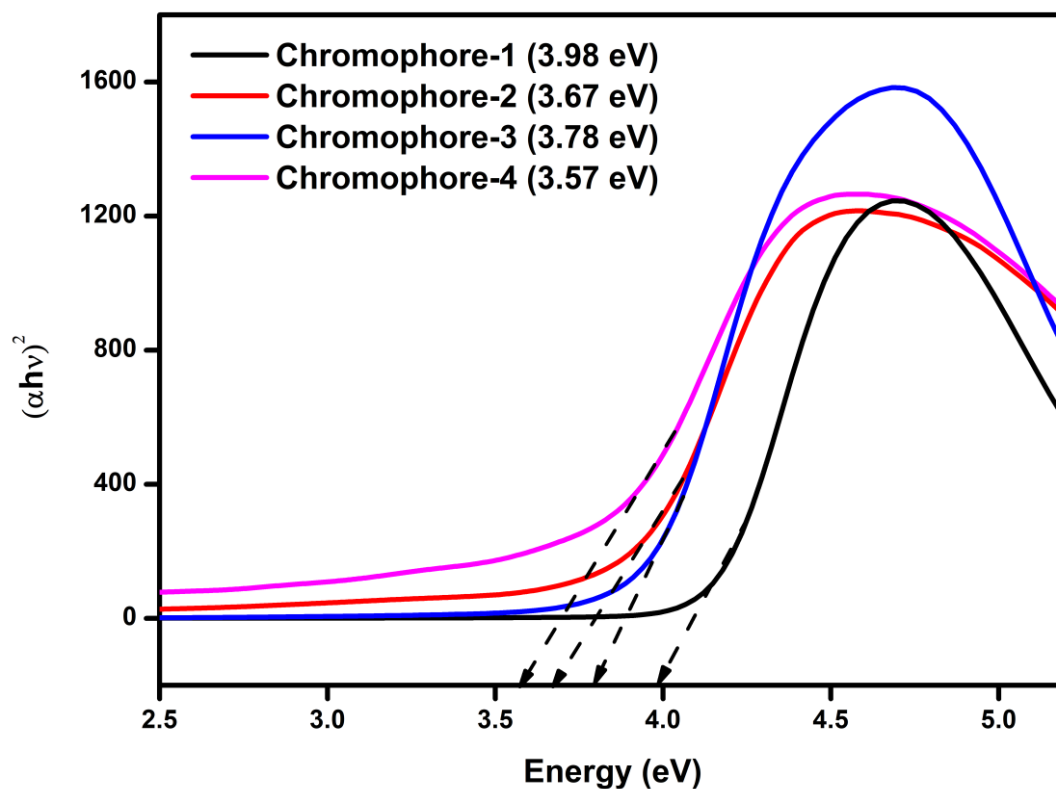


Fig. S18. Tauc plots of $(\alpha h\nu)^2$ versus photon energy $(h\nu)$ of chromophores 1-2.

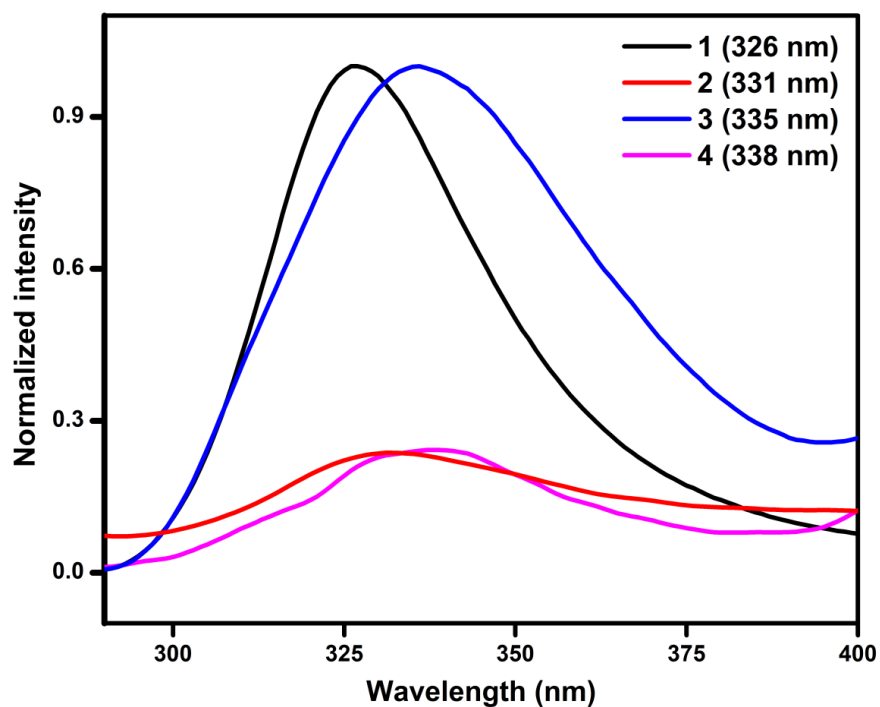


Fig. S19. Emission spectra of chromophores 1 - 4 in THF (1×10^{-5} M).

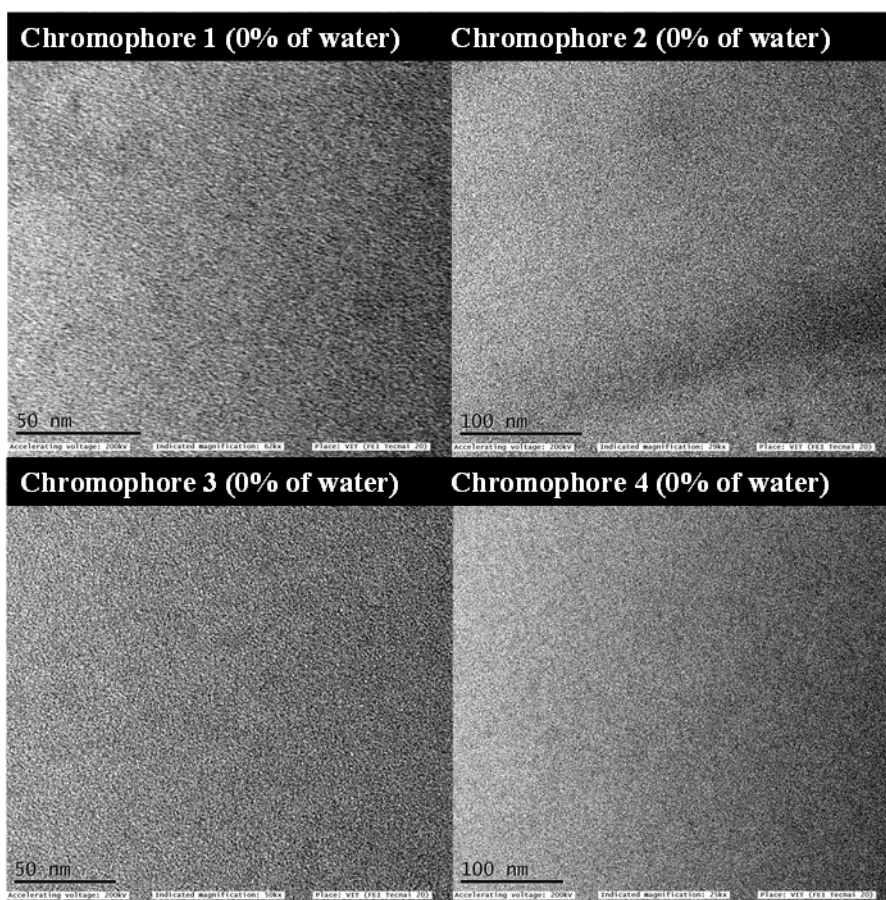


Fig. S20. The HR-TEM images of chromophores 1-4 indicate the no AIE dots at 0% of water.

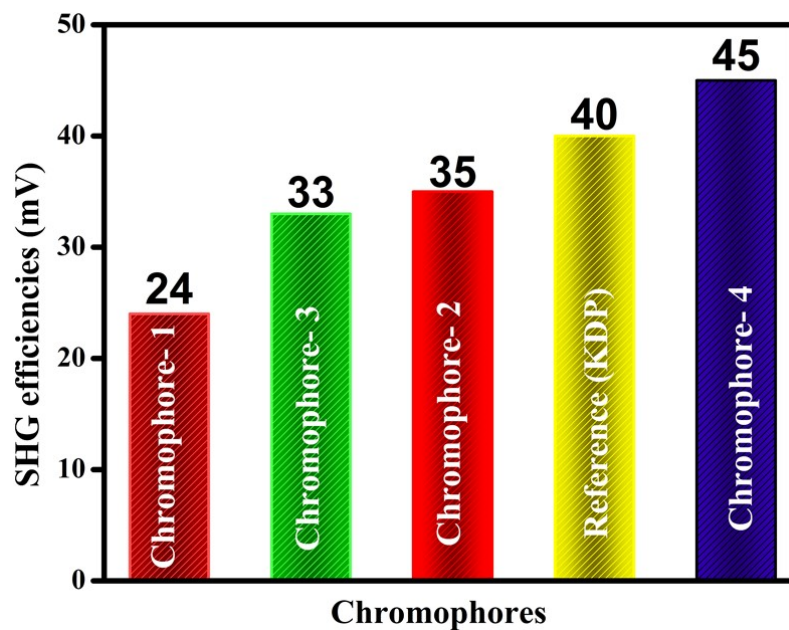


Fig. S21. SHG-NLO efficiency of chromophores 1-4 by Kurtz and Perry powder method.

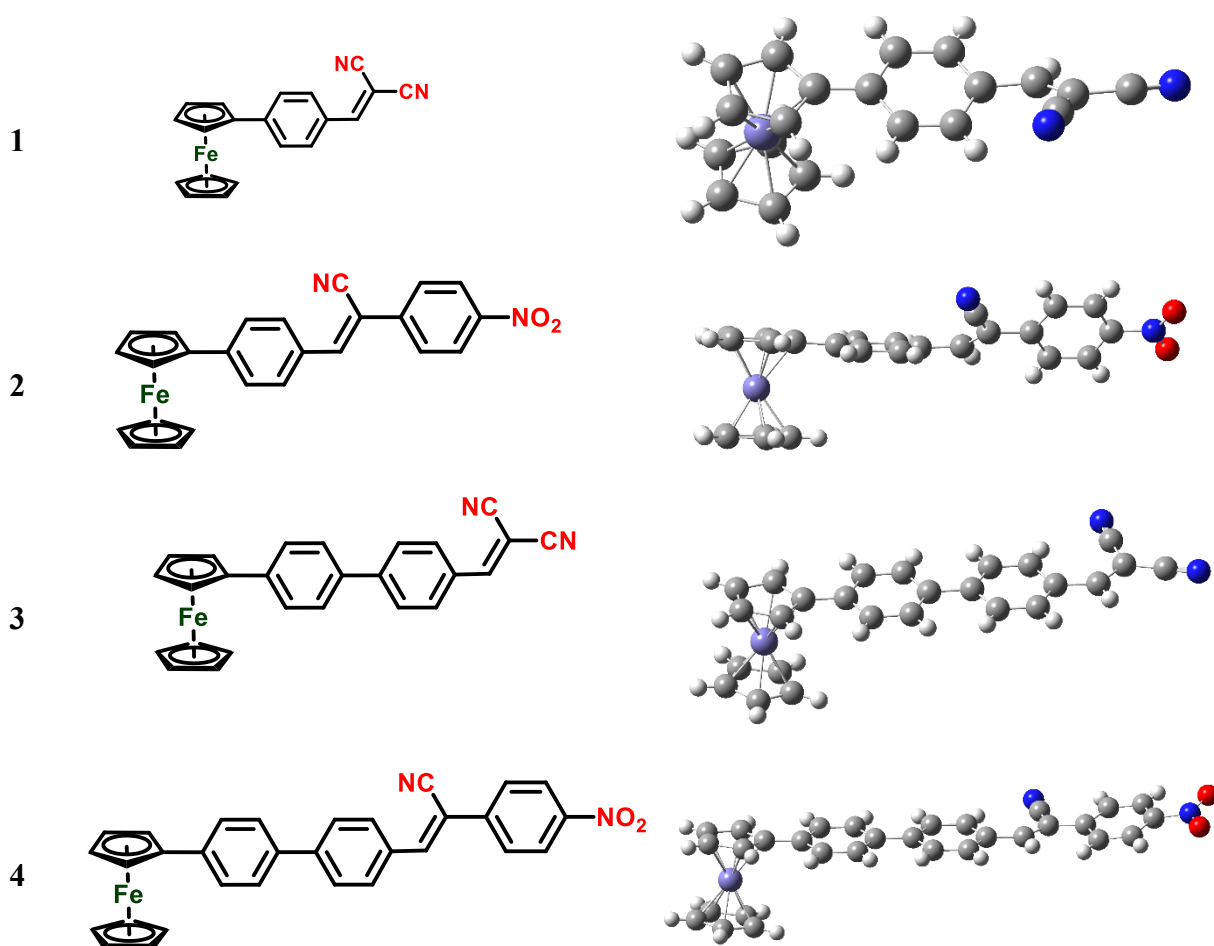


Fig. S22. The optimized geometry of chromophores 1-4 at B3LYP/6-31+G** level of theory.

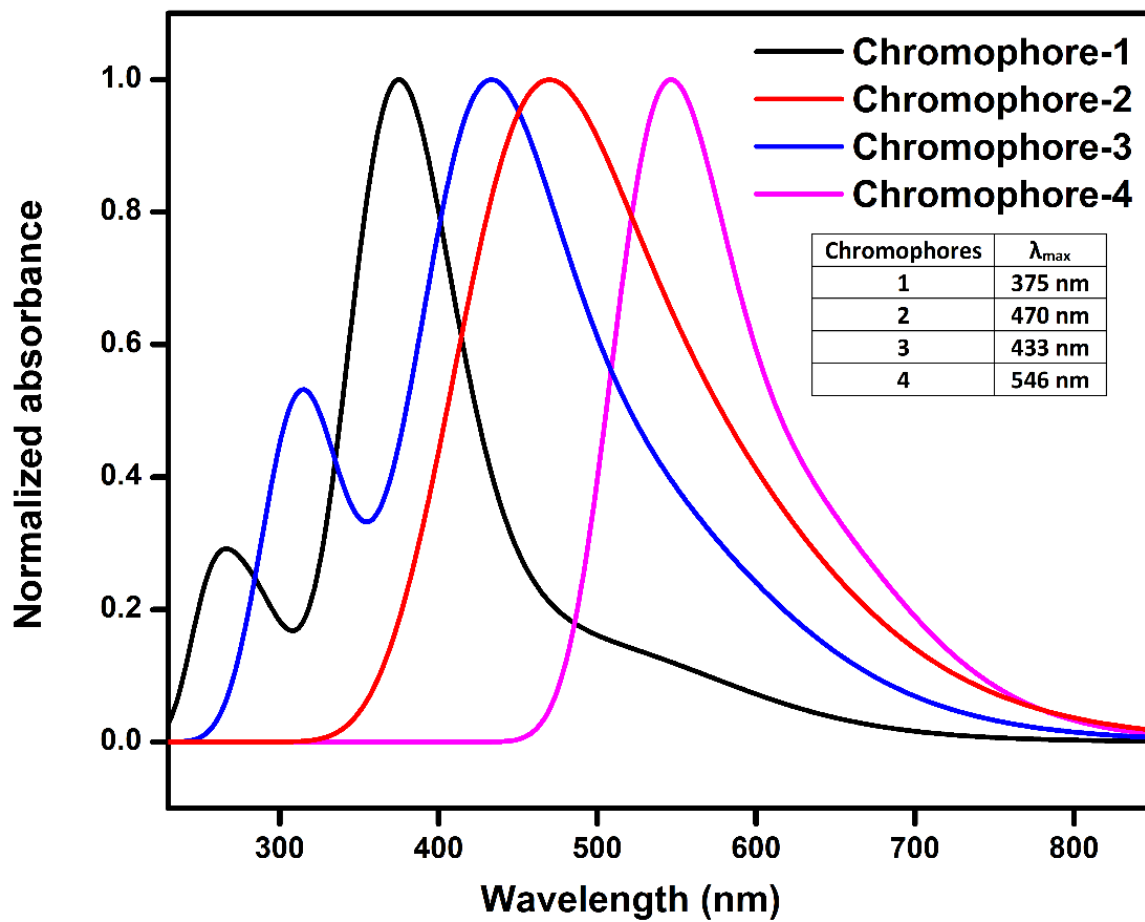


Fig. S23. UV-Visible spectrum of chromophores 1-4 was obtained CHCl_3 solvent by TD-DFT at B3LYP/6-31+G** level of theory.

Table S1. The data collections, structure refinement and parametric data of chromophores **2** and **4**.

	Chromophore 2	Chromophore 4
Empirical formula	C ₂₅ H ₁₈ Fe N ₂ O ₂	C ₃₁ H ₂₂ Fe N ₂ O ₂
Formula weight	434.26	510.35
Temperature	296(2) K	296(2) K
Wavelength	0.71073 Å	0.71073 Å
Crystal system, space group	Triclinic, P -1	Monoclinic, P c
Unit cell dimensions	a = 7.3724(9) Å alpha = 83.109(5) deg	a = 15.505(2) Å alpha = 90 deg
	b = 9.8599(14) Å beta = 84.277(5) deg	b = 5.9113(8) Å beta = 103.741(5) deg
	c = 13.615(2) Å gamma = 85.557(5) deg	c = 13.0683(13) Å gamma = 90 deg
Volume	975.5(2) Å ³	1163.5(3) Å ³
Z, Calculated density	2, 1.478 Mg/m ³	2, 1.457 Mg/m ³
Absorption coefficient	0.798 mm ⁻¹	0.681 mm ⁻¹
F(000)	448	528
Crystal size	0.350 x 0.350 x 0.300 mm	0.350 x 0.350 x 0.300 mm
Theta range for data collection	1.513 to 28.451 deg	1.352 to 28.305 deg
Limiting indices	-9<=h<=9, -13<=k<=13, - 14<=l<=18	-20<=h<=20, -7<=k<=7, 14<=l<=17
Reflections collected / unique	8004 / 4744 [R(int) = 0.0373]	9061 / 4352 [R(int) = 0.0340]
Completeness to theta = 25.242	99.0 %	99.8 %
Absorption correction	Semi-empirical from equivalents	Semi-empirical from equivalents
Max. and min. transmission	0.796 and 0.768	0.822 and 0.796
Refinement method	Full-matrix least-squares on F ²	Full-matrix least-squares on F ²
Data / restraints / parameters	4744 / 0 / 271	4352 / 2 / 325
Goodness-of-fit on F ²	0.769	1.080
Final R indices [I>2sigma(I)]	R1 = 0.0531, wR2 = 0.1448	R1 = 0.0379, wR2 = 0.0842
R indices (all data)	R1 = 0.0874, wR2 = 0.1815	R1 = 0.0522, wR2 = 0.1109
Extinction coefficient	n/a	n/a
Largest diff. peak and hole	0.323 and -0.481 e.Å ⁻³	0.254 and -0.291 e.Å ⁻³

Table S2. The selected bond angles, bond lengths and torsion angles of chromophores **2** and **4**.

Atoms	Chromophore 2	Atoms	Chromophore 4
Average Fe–C	2.039 (6)	Average Fe–C	2.047 (6)
Fe–Cent(1)	1.641 (3)	Fe–Cent(1)	1.655 (3)
Fe–Cent(2)	1.649 (3)	Fe–Cent(2)	1.661 (3)
Cent(1)–Fe(1)–Cent(2)	3.290 (4)	Cent(1)–Fe(1)–Cent(2)	3.315 (4)
C(1)–N(2)	1.460(12)	C(1)–N(2)	1.471(8)
C(8)–N(1)	1.137(7)	C(8)–N(1)	1.145(8)
N(2)–O(1)	1.224(10)	N(1)–O(1)	1.217(8)
N(2)–O(2)	1.266(10)	N(2)–O(2)	1.208(7)
C(2)–C(1)–N(2)	118.6(6)	C(2)–C(3)–N(1)	119.7(6)
C(6)–C(1)–N(2)	118.7(6)	C(4)–C(3)–N(1)	118.8(5)
N(1)–C(8)–C(7)	176.0(6)	N(2)–C(8)–C(7)	178.2(7)
O(1)–N(2)–O(2)	122.6(11)	O(1)–N(1)–O(2)	124.1(6)
C(1)–N(2)–O(1)	118.5(9)	C(3)–N(1)–O(1)	117.5(5)
C(1)–N(2)–O(2)	118.8(9)	C(3)–N(1)–O(2)	118.4(5)
N(2)–C(1)–C(2)–C(3)	178.7(6)	N(1)–C(3)–C(4)–C(5)	177.8(5)
C(4)–C(7)–C(9)–C(10)	179.4(5)	C(2)–C(1)–C(6)–C(7)	174.7(5)
C(4)–C(5)–C(6)–C(7)	179.7(5)	C(4)–C(5)–C(6)–C(7)	173.9(5)
C(9)–C(10)–C(11)–C(12)	176.3(5)	C(11)–C(12)–C(13)–C(16)	179.5(5)
C(16)–C(13)–C(14)–C(15)	178(5)	C(14)–C(13)–C(16)–C(17)	179.3(5)
C(15)–C(10)–C(9)–C(7)	148.3(6)	C(21)–C(20)–C(19)–C(22)	177.2(4)

Table S3. Solvatochromic data [$\tilde{\nu}_{max}$ (cm^{-1}) of the charge transfer band] for chromophores **1** - **4** in different solvents with α , β , π^* values by Kamlet and Taft.

Solvents	α	β	π^*	$\Delta\tilde{\nu}_{max}$							
				Absorption				Emission			
				1	2	3	4	1	2	3	4
Toluene	0.00	0.55	0.58	28.49	27.62	28.49	27.17	35.74	35.46	34.48	34.27
DEE	0.20	0.10	0.58	27.54	27.40	28.41	26.67	34.13	34.25	33.00	31.65
CHCl₃	1.00	0.66	0.69	27.40	27.47	28.45	26.66	33.78	33.90	31.55	31.45
THF	0.54	0.83	0.77	28.32	27.25	28.40	26.60	30.67	34.01	28.99	28.74
MeOH	0.83	0.75	0.62	27.55	27.40	28.41	27.03	32.90	35.21	28.82	33.00
ACN	0.35	0.4	0.75	27.32	26.95	28.32	26.52	27.93	32.89	34.25	28.99
DMF	0.88	0.00	0.69	27.54	26.81	27.85	26.53	27.78	31.45	28.49	28.41
DMSO	0.00	0.76	1.00	27.70	26.74	27.78	26.18	27.58	30.67	28.01	27.70

Where, α is the hydrogen bond donor strength (HBD), β is the hydrogen bond acceptor strength (HBA), and π^* corresponds to the dipolarity/polarizability of the solvent.

Table S4. Cyclic voltammetry data (potentials vs. FcH/FcH⁺), scan rate 100 mVs⁻¹ at the glassy carbon electrode of 0.5 mmolL⁻¹ solution of ferrocene and chromophores **1** - **4** in dry chloroform with 0.1 molL⁻¹ of nBu₄NClO₄ as the supporting electrolyte at 25 °C.

Chromophores	E _{pa} (mV)	E _{pc} (mV)	i _{pc} /i _{pa} (V)	E _{1/2} (mV)	ΔE (mV)
Ferrocene	509	438	0.98	473	71
1	639	359	0.66	499	278
2	692	340	0.80	516	352
3	756	361	0.75	558	395
4	761	423	0.69	592	338

Table S5. Fluorescence lifetime, quantum yield (non-aggregated and aggregated states), radiative and non-radiative parameters of chromophores **1** - **4**.

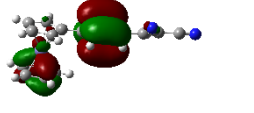
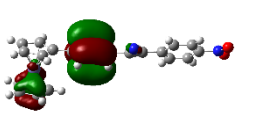
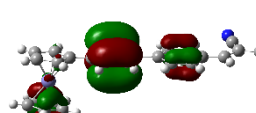
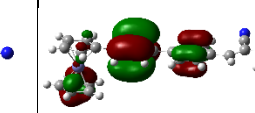

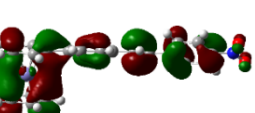
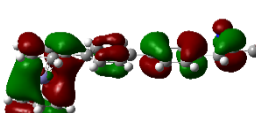

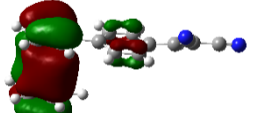
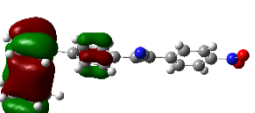
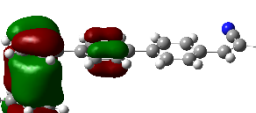
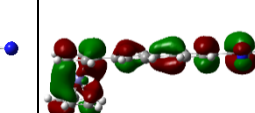
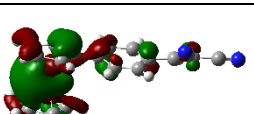
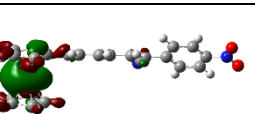
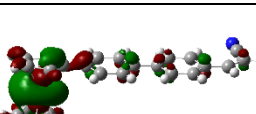
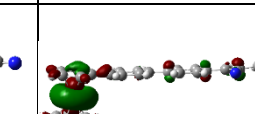
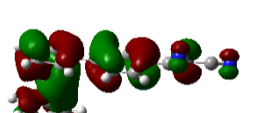
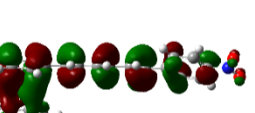
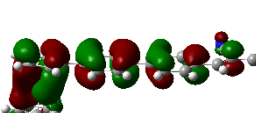
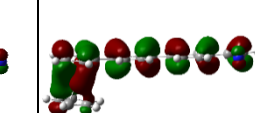
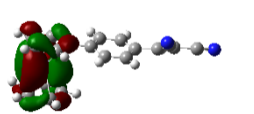
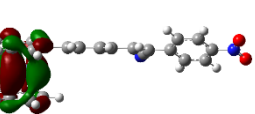
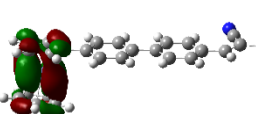
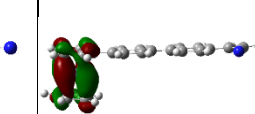
Chromophores	FL (λ _{max}) nm	τ (ns)	Φ [THF/ (THF: H ₂ O mixture)]	K _r (ns ⁻¹)	K _{nr} (ns ⁻¹)
1	326	2.01	0.023/ 0.273	0.011/ 0.135	0.486/ 0.362
2	331	3.61	0.029/ 0.344	0.008/ 0.095	0.269/ 0.182
3	335	2.93	0.031/ 0.351	0.011/ 0.175	0.331/ 0.222
4	338	5.30	0.045/ 0.480	0.008/ 0.091	0.180/ 0.098

Table S7. Selected transitions obtained from TD-DFT calculation with B3LYP/6-31+G** level theory of chromophores **1** - **4**.

S. No	λ _{max} (nm)	Oscillation strength, <i>f</i>	Energy (eV)	Selected major contributions
Chromophore-1	550	0.3226	2.25	H→L (83%)
	537	0.0614	2.31	H-1→L (41%)
	470	0.0191	2.64	H-1→L+4 (37%)
	441	0.0595	2.81	H→L+1 (36%)
	379	0.4044	3.27	H-2→L (72%)
	366	0.2742	3.38	H-3→L (63%)
	291	0.0290	4.25	H-5→L (64%)
	290	0.0591	4.26	H→L+1 (71%)
	256	0.1213	4.83	H-6→L (73%)
Chromophore-2	607	0.1410	2.04	H→L (81%)
	558	0.0138	2.22	H-1→L+6 (35%)
	481	0.6963	2.58	H-2→L (95%)
	437	0.1048	2.83	H→L+1 (88%)
	413	0.0214	2.99	H-3→L (90%)
	383	0.3738	3.23	H-4→L+1 (96%)
	376	0.1860	3.29	H-2→L+1 (59%)
	367	0.1733	3.37	H-2→L+1 (37%)
	313	0.0798	3.96	H-4→L+1 (23%), H-1→L+2 (26%)
Chromophore-3	566	0.1788	2.19	H→L (58%)
	499	0.1637	2.48	H-1→L+2 (35%)
	431	0.8276	2.87	H-2→L (95%)
	383	0.0951	3.24	H-3→L (74%)
	321	0.3103	3.87	H-5→L (67%)

	318	0.0747	3.89	H-6→L+1 (60%)
	306	0.0361	4.05	H-6→L+ (75%)
	293	0.0432	4.22	H-1→L+2 (71%)
	292	0.0570	4.24	H-5→L (74%)
Chromophore-4	586	0.2574	2.12	H→L (83%)
	524	0.0416	2.36	H-1→L+5 (21%), H→L+6 (24%)
	473	0.2454	2.62	H-2→L (29%)
	469	0.5406	2.64	H-3→L+5 (26%), H→L+5 (19%)
	416	0.1911	2.99	H→L+6 (81%)
	366	0.3947	3.39	H-1→L+1 (58%)
	360	0.1488	3.44	H-4→L (86%)
	352	0.1176	3.52	H-2→L+1 (34%)
	313	0.1042	3.96	H→L+2 (51%)
	283	0.1510	4.37	H-2→L+2 (44%)

Table S8. Density surface of the frontier orbitals involved in electronic transitions of Chromophores 1 - 4 which is derived from B3LYP/6-31+G** level of theory using iso-surface value of 0.02 au.

Orbitals	Chromophore-1	Chromophore-2	Chromophore-3	Chromophore-4
H-6				
H-5				
H-4				
H-3				
H-2				
H-1				

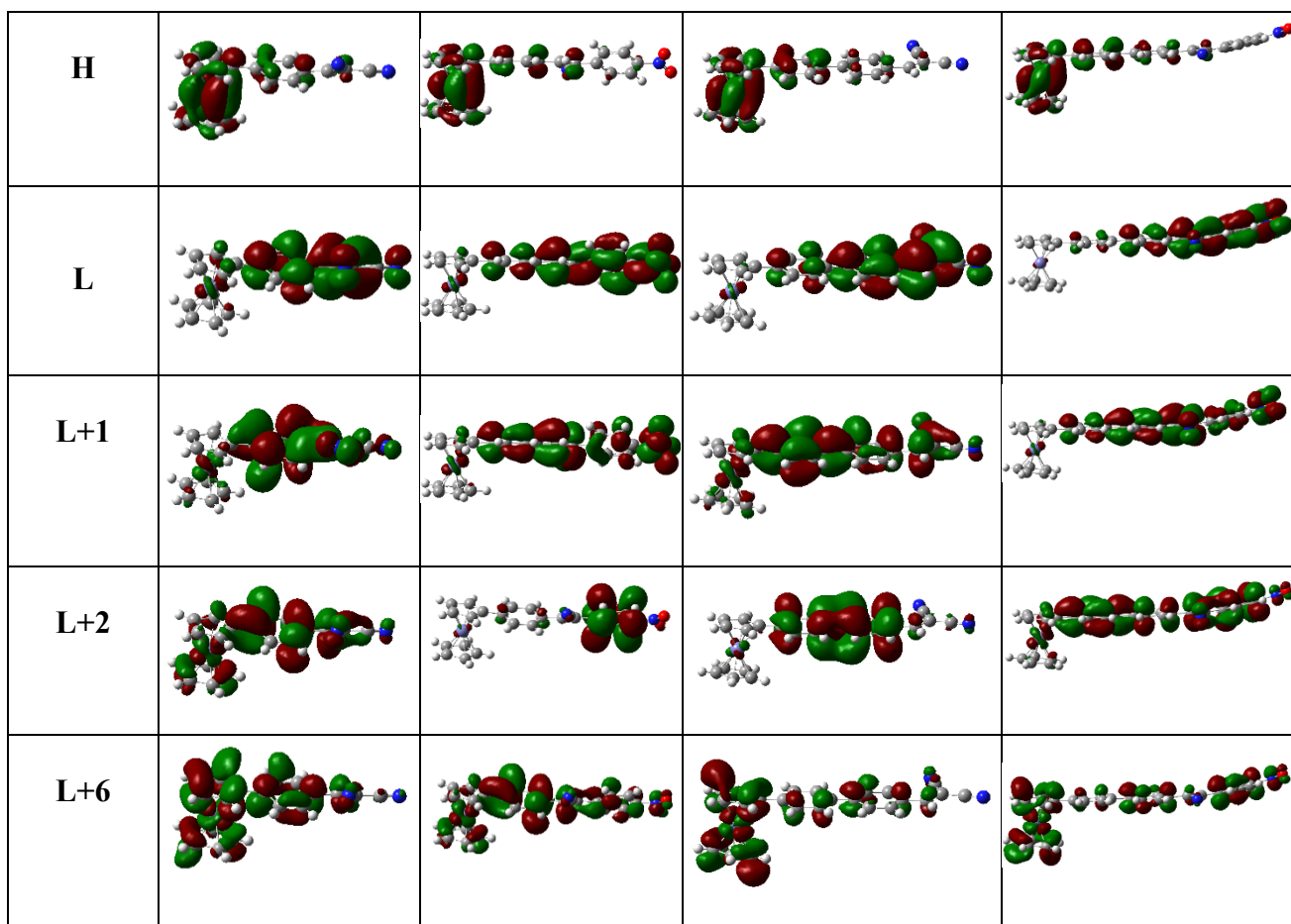


Table S9. Computed HOMO, LUMO energy gap, dipole moment and second-order nonlinear optical parameters of chromophores **1-4** using CAM-B3LYP/6-31+G** level of theory.

S. NO	E_{HOMO} (eV)	E_{LUMO} (eV)	Energy gap (eV)	μ_{total} (Debye)	α_0 ($\times 10^{-24}$ esu)	β_0 ($\times 10^{-30}$ esu)
1	-7.5835	-1.7317	5.852	7.82	25.587	5.538
2	-5.8515	-1.0537	4.798	8.39	37.012	23.653
3	-7.2640	-1.9039	5.360	8.79	35.463	13.009
4	-7.1378	-2.0365	5.101	8.62	44.734	19.783

Calculated HOMO, LUMO, energy gap and Polarizability (α_0) and Hyperpolarizability (β_0) using CAM-B3LYP/6-31+G** level of theory.

Table S10. Computed HOMO, LUMO energy gap, dipole moment and second-order nonlinear optical parameters of chromophores **1-4**) using LC-BLYP/6-31+G** level of theory.

S. NO	E _{HOMO} (eV)	E _{LUMO} (eV)	Energy gap (eV)	μ_{total} (Debye)	α_0 ($\times 10^{-24}$ esu)	β_0 ($\times 10^{-30}$ esu)
1	-9.0431	-0.7300	8.313	7.06	24.323	38.715
2	-8.6088	-0.9499	7.659	7.63	32.082	62.569
3	-8.7854	-0.9279	7.858	8.42	33.248	82.503
4	8.4393	-1.0920	7.347	8.25	41.538	113.570

Calculated HOMO, LUMO, energy gap and Polarizability (α_0) and Hyperpolarizability (β_0) using LC-BLYP/6-31+G** level of theory.

Reference

- [1] (a) D. Zhang, L. Zhu, H. Li, J. Su, *Front. Chem. China*. 2010, **5**, 241–6. (b) R. Zhang, Z. Wang, Y. Wu, H. Fu, J. Yao, *Org. Lett.* 2008, **10**, 3065–8.
- [2] V. S. Subiksha, T. Viswanathan, E. David, S. Prabu, N. Palanisami, *Spectrochim. Acta - Part A Mol Biomol Spectrosc.* 2022, **277**, 121282.
- [3] W. Clegg, A. J. B. R. O. G PM, *Crystal Structure Analysis Principles and Practice*, **2001**.
- [4] A. J. Blake, J. M. Cole, J. S. O. Evans, P. Main, S. Parsons, D. J. Watkin, *Crystal structure analysis: principles and practice*, OUP Oxford, **2009**.
- [5] G. M. Sheldrick, *Acta Crystallogr Sect A Found Crystallogr.* 2015, **71**, 3–8.
- [6] X. Xu, L. Li, B. Liu, Y. Zou, *Appl. Phys. Lett.* 2011 **98**, 25.
- [7] M. J. Frisch, G. W. Trucks, H. B. Schlegel, G. E. Scuseria, M. A. Robb, J. R. Cheeseman, G. Scalmani, V. Barone, B. Mennucci, G. A. Petersson, H. Nakatsuji, M. Caricato, X. Li, H. P. Hratchian, A. F. Izmaylov, J. Bloino, G. Zheng, J. L. Sonnenberg, M. Hada, M. Ehara, K. Toyota, R. Fukuda, J. Hasegawa, M. Ishida, T. Nakajima, Y. Honda, O. Kitao, H. Nakai, T. Vreven, J. A. Montgomery, Jr., J. E. Peralta, F. Ogliaro, M. Bearpark, J. J. Heyd, E. Brothers, K. N. Kudin, V. N. Staroverov, R. Kobayashi, J. Normand, K. Raghavachari, A. Rendell, J. C. Burant, S. S. Iyengar, J. Tomasi, M. Cossi, N. Rega, J. M. Millam, M. Klene, J. E. Knox, J. B. Cross, V. Bakken, C. Adamo, J. Jaramillo, R. Gomperts, R. E. Stratmann, O. Yazyev, A. J. Austin, R. Cammi, C. Pomelli, J. W. Ochterski, R. L. Martin, K. Morokuma, V. G. Zakrzewski, G. A. Voth, P. Salvador, J. J. Dannenberg, S. Dapprich, A. D. Daniels, Ö. Farkas, J. B. Foresman, J. V. Ortiz, J. Cioslowski, D. J. Fox, *Gaussian 16, Revision C.01*, Gaussian, Inc., Wallingford CT. **2016**.
- [8] D. Roy, A. K. Todd, M. M. John, *GaussView, Version 6.1*. Semichem Inc. **2016**, Shawnee Mi..
- [9] M. Gopalakrishnan, K. Thirumoorthy, N.S.P. Bhuvanesh, N. Palanisami, *RSC Adv.* 2016, **6**, 55698–55709.

- [10] H. Saeidian, M. Sahandi, *J. Mol. Struct.* 2015, **1100**, 486–495.
- [11] R.T. Lynch Jr, M.D. Levenson, N. Bloembergen, *Phys. Lett. A.* 1974, **50**, 61–62.